Latin American Journal of Solids and Structures
www.lajss.org

An isotropic damage model to simulate collapse in reinforced concrete elements

Abstract

A damage model with different failure surface in tension and compression is formulated, implemented and validated to study reinforced concrete elements under actions which induce their collapse. The constitutive behaviour of concrete considers the softening deformation after reaching a failure surface, whereas the hardening of the reinforcing steel is represented by a plasticity von Mises surface. The developed damage model does not exhibit the problem of stress locking as the smeared cracking model does; this guaranties an adequate energy release as the material fails. Numerical examples are presented showing the validity of the developed damage model for modelling the behaviour of reinforced concrete elements up to their collapse.

Keywords

Damage, constitutive models, failure, degradation.

Juárez-Luna G. [a,*]
Méndez-Martínez H.[a,1]
Ruiz-Sandoval M.E.[a,2]

[a] Universidad Autónoma Metropolitana, San Pablo No. 180, Col. Reynosa Tamaulipas, 02200 México, D.F. Telephone: (55) 5318-9085; Fax: (55)5318-9085;

[*] gjl@correo.azc.uam.mx,
[1] ic_hmm@hotmail.com,
[2] mrh@correo.azc.uam.mx

Received 22.01.2014
In revised form 16.05.2014
Accepted 03.06.2014
Available online 17.08.2014

1 INTRODUCTION

The simulation of structures in their evolution to collapse is an interesting topic in engineering to know the remaining capacity of a structure after reaching the ultimate load, which is dependent on the constitutive behaviour of their construction materials. After concrete reaches its ultimate load, it presents a reduction of its load-carrying capacity, so the stresses decreases while the strains increases; this behaviour is typically called strains softening.

The continuum damage mechanics can be used for modelling concrete failure, one of the pioneers of damage mechanics theory was Kachanov (1958), who introduced the fundamental concepts of the continuous damage mechanics, *i.e.*, effective strain, effective stress and scalar damage variable. There are many local damage models based on the damage framework such as: isotropic damage models (Kachanov 1958, Krajcinovic 1984, 1985, Lemaitre 1986, Simo and Ju 1987a, Lubliner *et al.* 1989, Mazars and Pijaudier-Cabot 1989, Lubarda *et al.* 1994, Faria *et al.* 1998, Lee and Fenves

1998, Comi 2001, Jason *et al.* 2006, Contrafatto and Cuomo 2006, Wu *et al.* 2006 and Gopinath *et al.* 2012); anisotropic damage models (Dragon and Mroz 1979, Cordebois and Sidoroff 1979, Krajcinovic and Fonseka 1981, Ortiz 1985, Simo and Ju 1987a, b, Ju 1989, 1990, Voyiadjis and Abu-Lebdeh 1994, Govindjee *et al.* 1995, Halm and Dragon 1996, Fichant *et al.* 1999, Lemaitre *et al.* 2000, Carol *et al.* 2001 and Cicekli *et al.* 2007).

It is well kwon that local continuum damage models lead to a physically unrealistic description of the strain localization phenomenon. When the tangent stiffness matrix is not positive definite, the governing differential equations may lose ellipticity, which renders the boundary value problem ill posed (Needleman 1988, Jirásek 1998). In finite elements computations spurious mesh sensitivity problems occur, strain localizes into a narrow band whose width depends on the element size, the corresponding load-displacement curve always shows snapback for a fine mesh and the dissipate fracture energy converges to zero. To overcome the shortcomings of local theories for modelling strain softening, some alternatives have been proposed such as: non-local modelling of the constitutive behaviour (Costa Mattos *et al.* 1992, Costa Mattos and Sampaio 1995, Da Costa Mattos *et al.* 2009), gradient material description (Triantafylidis and Aifantis 1986, Peerlings *et al.* 1996), micropolar continuum theory (de Borst 1991, Steinmann 1995), viscous regularization (de Borst and Mühlhaus 1992) and local manipulations of the material properties depending on the element size (Bazant and Oh 1983, Crisfield 1986, Oliver 1989). Recently, Da Costa-Mattos *et al.* (2009) proposed a special gradient-enhanced damage theory in which the material is considered to possess a substructure or microstructure, where the free energy is supposed to depend not only on the strain and the damage variable but also on the damage gradient.

If the concrete is modelled with the finite element method and local damage models, the damage of a cracking surface is distributed into the material volume of a finite element, which is inconsistent with the fracture energy dissipated per unit of area and per unit of volume. This disagreement is overcome with a characteristic length such as the proposed one by Bazant and Oh (1983), who used a thickness of the cracking band, depending on the element area and on the propagation direction; Crisfield (1986) proposed a characteristic length defined by the Jacobian in each integration point; and Oliver (1989) developed a general method for computing the characteristic length depending on the element size and the elastic stress state.

The Software Ansys 12.0 uses a damage surface for concrete with different threshold values under tension and compression, coherent with the behaviour reported in laboratory test such as Kupfer and Gerstle (1973). However, this model has as a drawback that fracture energy has a fixed value, which is not possible to modify, so the results are dependent on that fixed energy fracture. Also, Ansys only considers linear softening curve, even though there are other curves with a better approximation such as bilinear, trilinear and exponential. Alternatively, the Software Diana 9.0 uses the smear cracking model for concrete (Rashid 1968, Rots 1988), in which is possible to assign the value of the fracture energy density. Nevertheless, this model has problems of mesh dependency, stress locking and spurious kinematic modes.

In the attempt to simulate material failure by mesh independent models, Hillerborg *et al.* (1976) developed the discrete crack model, where a previous stress analysis must be performed to a priori localize the strain concentration zones, where interfaces are placed on the boundaries of the elements, bringing about that the results are mesh dependent. Another alternative to simulate materi-

al failure is the strain localization model (Simo *et al.* 1993, Oliver 1996a, 1996b, Armero and Garikipati 1996, Juárez and Ayala 2009, Juárez-Luna and Ayala 2014), which considers that only one discontinuity (crack) may propagate into a finite element, so in the case that multi cracks appears, the computational cost of their propagation is high.

For the aforementioned reasons, this paper promotes the use of continuous damage models, which do not need computational costly tracking algorithms. A continuous damage model is developed and implemented to simulate the constitutive behaviour of the concrete in its evolution to collapse. This damage model, called different tension-compression (DTC), has a failure surface with the corresponding threshold values in tension and compression of the concrete. Additionally, in this model, it is possible to assign the density energy magnitude and it does not have the problems reported by Rots (1988).

The proposed DTC damage model uses the failure surface proposed by Oliver *et al.* (1990). Nevertheless, the tangent constitutive tensor is different to the one developed by Linero (2006). The DTC damage model was implemented into the subroutines of the Finite Element Analysis Program (FEAP) (Taylor 2008), then it was validated with the numerical reproduction of numerical examples and experimental reinforce concrete tests reported in the literature. It is important to mention that in this paper, the material failure is represented by a isotropic damage variable, which represents the degradation level, so the material degradation into the finite element analyses is presented as localization zones where important displacements occurs, but not as physical discontinuities (cracks).

2 DAMAGE MODEL FORMULATIONS

2.1 Equal tension-compression

The isotropic continuum damage model by Simo and Ju (1987a) and Oliver *et al.* (2002) with a failure surface equal tension-compression (ETC) is shown in
Figure 1 for 1D and 2D problems, where the ultimate tensile and compressive strength, σ_{ut}, and, σ_{uc}, respectively, have the same magnitude. This model, typically used to simulate the constitutive behaviour of some metals, is defined by the following equations:

$$
\begin{aligned}
&\text{a)}\ \text{Free energy density} && \Psi\left(\boldsymbol{\varepsilon}, r\right) = \left(1 - d(r)\right)\Psi_0 \\
&\text{b)}\ \text{Constitutive equation} && \boldsymbol{\sigma} = \frac{\partial \Psi}{\partial \boldsymbol{\varepsilon}} = (1-d)\mathbf{C} \,:\, \boldsymbol{\varepsilon} \\
&\text{c)}\ \text{Damage variable} && d\left(r\right) = 1 - \frac{q}{r};\quad q \in \left[r_0, 0\right]\quad d \in \left[0,1\right] \\
&\text{d)}\ \text{Evolution law} && \dot{r} = \gamma \begin{cases} r \in \left[r_0, \infty\right] \\ r_0 = r\big|_{t=0} = \frac{\sigma_y}{\sqrt{E}} \end{cases} \\
&\text{e)}\ \text{Damage criterion} && f(\tau_\sigma, q) = \tau_\sigma - q = \sqrt{\boldsymbol{\sigma} : \mathbf{C}^{-1} : \boldsymbol{\sigma}} - q; \begin{cases} q \in \left[0, r_0\right] \\ q\big|_{t=0} = r_0 \end{cases} \\
&\text{f)}\ \text{Hardening rule} && \dot{q} = H^d\left(r\right)\dot{r};\quad H^d\left(r\right) = q'\left(r\right) \le 0 \\
&\text{g)}\ \text{Loading-unloading conditions} && f < 0;\quad \gamma \ge 0;\quad \gamma f = 0;\quad \gamma \dot{f} = 0 \ \text{(consistency)}
\end{aligned}
\tag{1}
$$

where Ψ is the free energy density, ε is the strain tensor, $\boldsymbol{\sigma}$ is the stress tensor and $\mathbf{C}$ is the elastic tensor. The damage variable, d, is defined in terms of hardening/softening variable q, which is dependent on the hardening/softening parameter, H. The damage multiplier γ determine the loading-unloading condition, the function, $f(\tau_\sigma, q)$, bounds the elastic domain defining the damage surface in the stress space. The value, r_o, is the threshold that determines the limit of the initial elastic domain, *i.e*, $q=r_o$. In this ETC damage surface, any stress state is transformed to a norm, bounded by r_o, where every stress state outside of this circle is inelastic as shown in
Figure **2**.

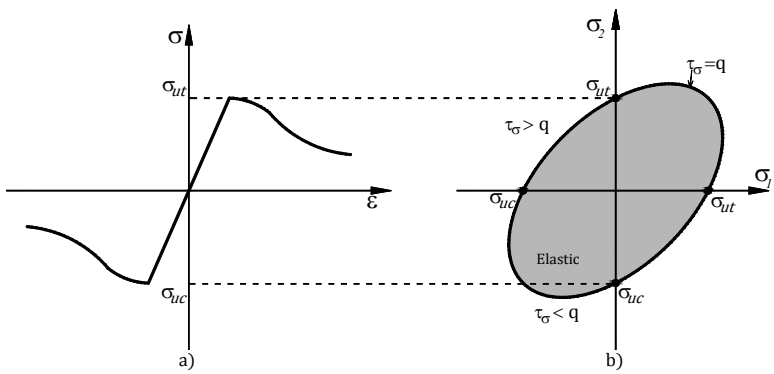

Figure 1: ITC model: a) 1D behaviour and b) 2D failure surface.

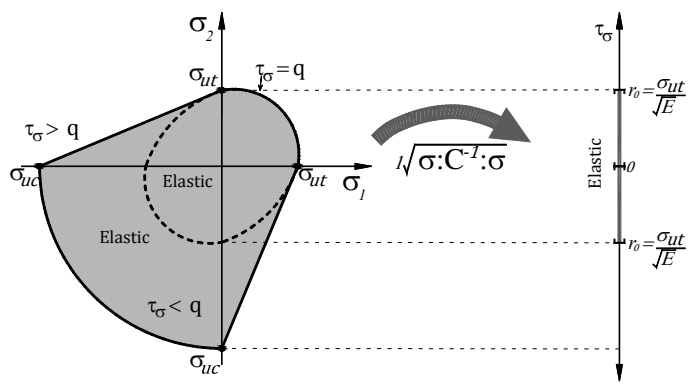

Figure 2: Transformation of the stress state to a norm.

The tangent constitutive equation, in terms of rates, from the model in Eq. (1) is:

$$\dot{\boldsymbol{\sigma}} = \mathbf{C}^T : \dot{\boldsymbol{\varepsilon}} \tag{2}$$

Where $\mathbf{C}^T$ is the continuum tangent constitutive operator, relating the stress and the strains rates, of the nonlinear loading interval, which is defined by

$$\mathbf{C}^T = (1-d)\mathbf{C} - \frac{q - H_r}{r^3}(\mathbf{C} : \boldsymbol{\varepsilon} \otimes \boldsymbol{\varepsilon} : \mathbf{C}) \tag{3}$$

and for the elastic loading and unloading interval($\dot{d} = 0$):

$$\mathbf{C}^T = \left(1 - d\right)\mathbf{C} \tag{4}$$

2.2 Different tension-compression

The formulation of the damage model with failure surface DTC is based on the ETC damage model. The main difference of this model is the definition of the norm, which is modified for a parameter proposed by Lubliner *et al.* (1989). It is well known that concrete has a ratio between the compression and tension strength of 10 to 20, *i.e.*, $n=\sigma_{uc}/\sigma_{ut}$, as shown in Figure 3. To have a failure surface with that characteristic, the norm given in Eq. (1)e, is modified by the parameter χ, then

$$f(\tau_\sigma, q) = \chi\tau_\sigma - q = \chi\sqrt{\boldsymbol{\sigma} : \mathbf{C}^{-1} : \boldsymbol{\sigma}} - r \tag{5}$$

Also, the tangent constitutive tensor, $\mathbf{C}^T$, for the nonlinear interval is:

$$\mathbf{C}^T = (1 - d)\mathbf{C} - \frac{q - H_r}{r^3}\chi^2(\mathbf{C} : \boldsymbol{\varepsilon} \otimes \boldsymbol{\varepsilon} : \mathbf{C}) \tag{6}$$

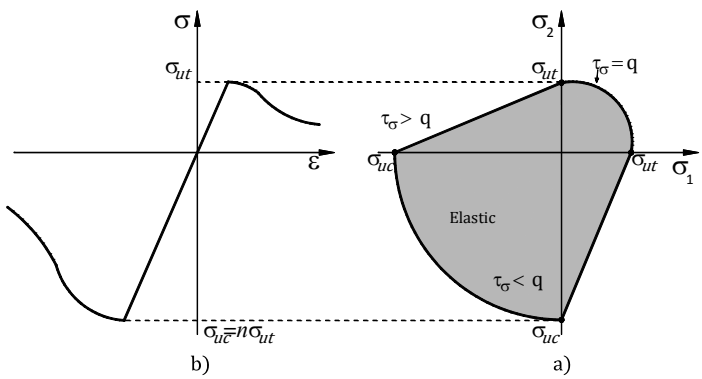

Figure 3: Constitutive behaviour of plain concrete: a) 1D and b) 2D

The parameter χ in Eqs. (5)

$$\chi = \phi + (\frac{1 - \phi}{n}) \tag{7}$$

where ϕ a is weight factor, depending on the principal stresses, σ_i, given by:

$$\phi = \frac{\sum_{i=1}^{3} \langle \sigma_i \rangle}{\sum_{i=1}^{3} |\sigma_i|} \tag{8}$$

Where the Maclauy $\langle\rangle$ operator and the symbol || consider, respectively, the positive and the absolute magnitudes of the principal stresses. The interval of ϕ is $[0,1]$, bounded by 0 for a triaxial compression ($\sigma_3 \leq \sigma_2 \leq \sigma_1 \leq 0$) and 1 for triaxial tension ($0 \leq \sigma_3 \leq \sigma_2 \leq \sigma_1$). Consequently, the corresponding interval of χ is $[1/n,1]$, bounded by $1/n$ for a triaxial compresion and 1 for triaxial tension.

The parameter χ scales down $1/n$ times the norm, as shown in Figure 4, in such a way it is compared with the elastic interval $[0,r_o]$. The value of $r_o=\sigma_{ut}/\sqrt{E}$ depends on the threshold value of σ_{ut} and the Young's modulus E. Note that the initial elastic interval is the same for 1D, 2D and 3D problems, all with a limit point r_o, and that for a 2D principal stress state, the parameter χ takes the value of 1 in the firts quadrant, $1/n$ in the third quadrant and the interval $[1/n,1]$ in the second and fourth quadrants.

The algorithm to implement the DTC damage model is as follows:

1. Initial data

   Material properties: n, G_f, σ_{ut},
   Current values: ε_{t+1}, d_{t+1}, r_{t+1}

2. Evaluate the effective stresses and norm

$$\begin{aligned} \bar{\boldsymbol{\sigma}}_{t+1} &= \mathbf{C} \;:\; \boldsymbol{\varepsilon}_{t+1} \\ \tau_{t+1} &= \chi \sqrt{\bar{\boldsymbol{\sigma}}_{t+1} : \mathbf{C}^{-1} : \bar{\boldsymbol{\sigma}}_{t+1}} \end{aligned} \tag{9}$$

3. Identification of state (if t=0, then $r_0 = \sigma_{ut} / \sqrt{E}$):

   a) If $\tau_{t+1} \leq r_t$, the elastic/unload/neutral load case, then

$$\begin{aligned} r_{t+1} &= r_t \\ d_{t+1} &= 1 - \frac{q(r_t)}{r_t} \\ \mathbf{C}_{t+1}^{T} &= \left(1 - d_{t+1}\right)\mathbf{C} \\ \boldsymbol{\sigma}_{t+1} &= (1 - d_{t+1})\bar{\boldsymbol{\sigma}}_{t+1} \end{aligned} \tag{10}$$

b) If $\tau_{t+1} > r_t$, the load case, then

$$
\begin{aligned}
r_{t+1} &= \tau_{t+1} \\
d_{t+1} &= 1 - \frac{q(r_{t+1})}{r_{t+1}} \\
\mathbf{C}^{T}_{t+1} &= \left(1 - d_{t+1}\right)\mathbf{C} - \frac{q - Hr_{t+1}}{r^{3}_{t+1}}\chi^{2}\left(\bar{\boldsymbol{\sigma}}_{t+1} \otimes \bar{\boldsymbol{\sigma}}_{t+1}\right) \\
\boldsymbol{\sigma}_{t+1} &= (1 - d_{t+1})\bar{\boldsymbol{\sigma}}_{t+1}
\end{aligned}
\tag{11}
$$

4. Output values: r^{t}, $\mathbf{C}^{\mathrm{T}}$ and σ^{t+1}.

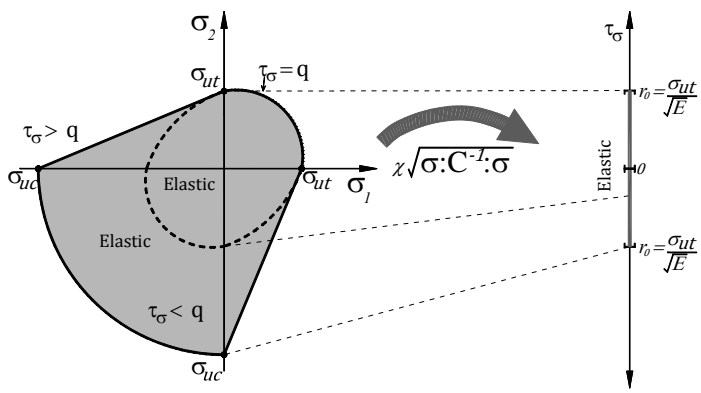

Figure 4: Transformation of the stresses to a norm.

Note that if the value of $\chi=1$ in the norm and in the tangent constitutive tensor, the ETC continuous damage model is recovered. An equivalent way of evaluate the damage criterion is proposed, modifying the threshold value of r_o in the limit point for the value of $r_{om}=r_o/\chi$. With this modification, in a 2D principal stress state, the value of r_o is scaled up *1* time in the first quadrant, n times in the third quadrant and *1* to *n* times in the second and fourth quadrants, as shown in Figure 5. Then, the algorithm for the ETC continuous damage needs only a modification in the threshold value of r_o. Both ways of the DTC continuous damage model were implemented in the user routines of FEAP, having the same results.

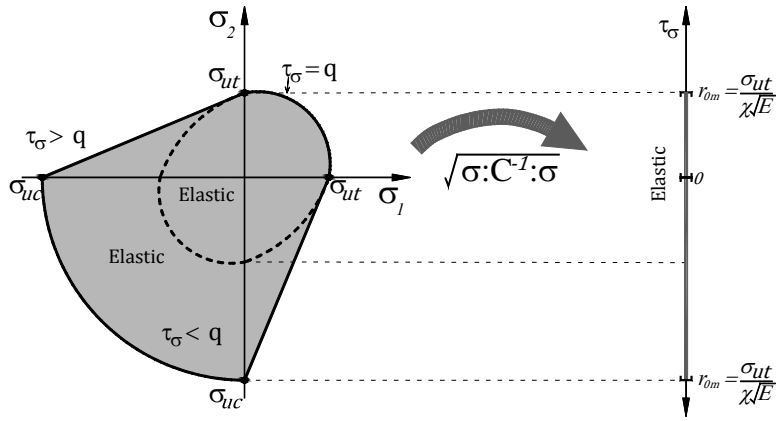

Figure 5: Transformation of the stresses to a norm with a modified r_0.

3 NUMERICAL EXAMPLES

In the three presented examples, the reinforcement was meshed with 3D linear elements with two nodes equipped with three degrees of freedom. The constitutive behaviour of the steel reinforcement was modelled with a plasticity surface of von Mises. The steel elements were placed on the boundary of the solid elements, coupling the degree of freedom of both kinds of elements and then perfect bond was considered. This DTC damage model was validated for plain concrete elements in Méndez-Martínez and Juárez-Luna (2012).

3.1 Lightly reinforced concrete beam

In this example, a simple supported concrete beam is analysed, the dimensions of the reinforcement and boundary conditions are shown in Figure 6. A load is applied at the centre of the span by displacement control, which is gradually imposed downwards. The mechanical properties of the concrete are: Young's modulus, $Ec=24132\ MPa$, Poisson ratio $\nu=0.2$, ultimate tensile strength compressive $\sigma_{tu}=2.41\ MPa$, ultimate compressive strength $\sigma_{cu}=33.23\ MPa$ and fracture energy density $G_f=0.263\ N/mm$. The mechanical properties of the steel reinforcement are: Young's modulus, $E_s=203.4\ GPa$, yield stress $\sigma_y=324\ MPa$, Poisson ratio $\nu=0.3$, area $A=5.07\ cm^2$, hardening modulus $H=6.9\ GPa$ and strain at which tensile strength is achieved 10%.

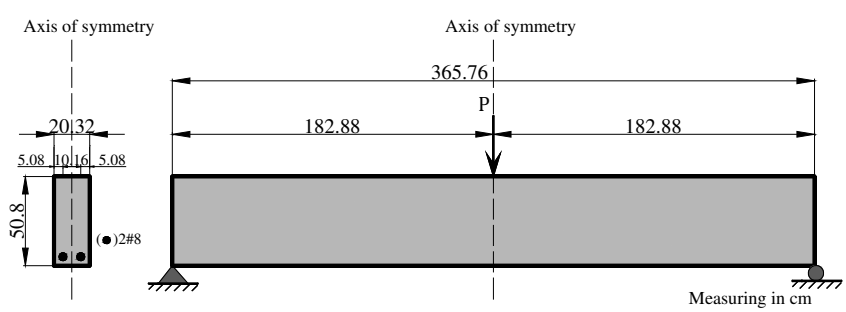

Figure 6: Geometry and reinforcement.

The beam was meshed with hexahedral elements as shown in Figure 7a, where only a quarter of the beam was modelled because of its symmetry, reducing the time consuming of the computational cost. As can be seen, the failure started into the finite elements placed around the centre on the span, at the bottom of the beam as shown in Figure 7b, which is coherent with the experimental results reported by Burns and Seiss (1962). The load *vs.* displacement curves at the centre of the span are shown in Figure 8, where the curve computed with the DTC damage model is acceptable with the curve reported by Burns and Seiss (1962), showing the validity of the implemented DTC damage model to simulate reinforced concrete elements.

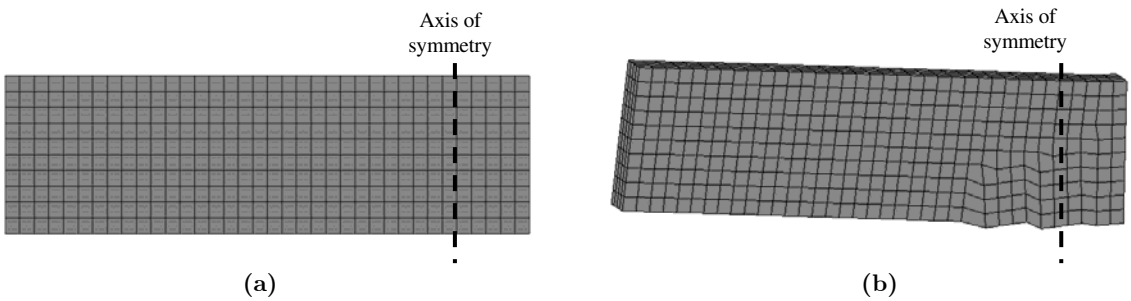

Figure 7: Mesh: a) undeformed and b) deformed

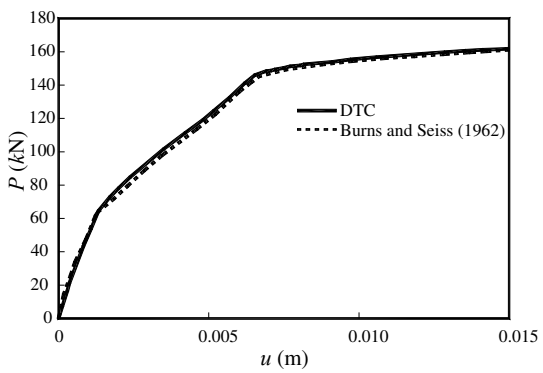

Figure 8: Load *vs.* displacement curves.

3.2 Reinforced concrete circular slab

In this example, a reinforced concrete slab with circular shape was studied, in which a distributed uniform load is gradually applied downwards. Two boundary conditions were considered at the border of the slab, simple supported and fixed. The geometry and reinforcement of the slab with thickness of *0.10 m* are shown in
Figure 9. The mechanical properties of the concrete are: Young's modulus E_c=*14710 MPa*, Poisson ratio ν=*0.2*, ultimate tensile strength σ_{tu}=*2.45 MPa*, ultimate compressive strength σ_{cu}=*29.42 M Pa* fracture energy density G_f=*0.098 N/mm*. The mechanical properties of the steel reinforcement are: Young's modulus E_s=*196.13 MPa*, yield stress σ_y=*411.88 MPa*, Poisson ratio ν=*0.3*, area A=*0.71* cm^2 and hardening modulus H=*2.871 GPa*.

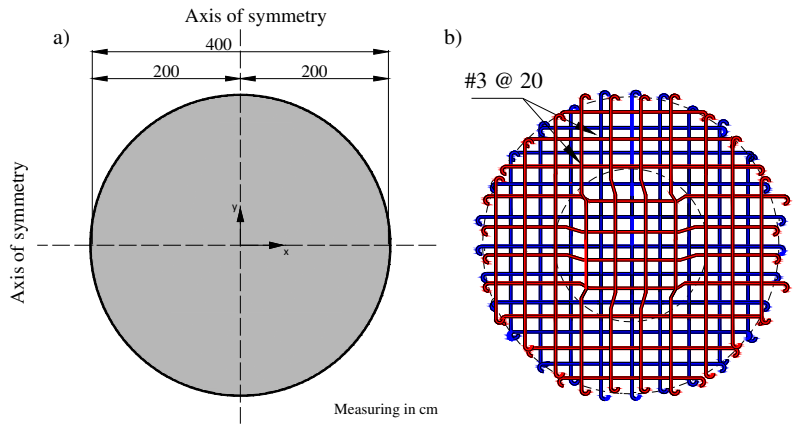

Figure 9: Circular slab: a) geometry and b) reinforcement.

As the previous example, the two axes or symmetry were considered, so only a quarter of the slab was modelled with hexahedral elements, as shown in Figure 10a, to reduce the time consuming of the computational calculation. The undeformed meshes are shown in Figure 10b and c, for the simple supported and fixed at the border of the slab, respectively.

The load *vs.* displacements curves are shown in Figure 11a and b for simple supported and fixed conditions, respectively. These curves are compared with those reported by Caballero (2012), computed by a smear crack model in the Software ANSYS. As can be seen, both computed curves are coherent with those simulated with a smear crack model.

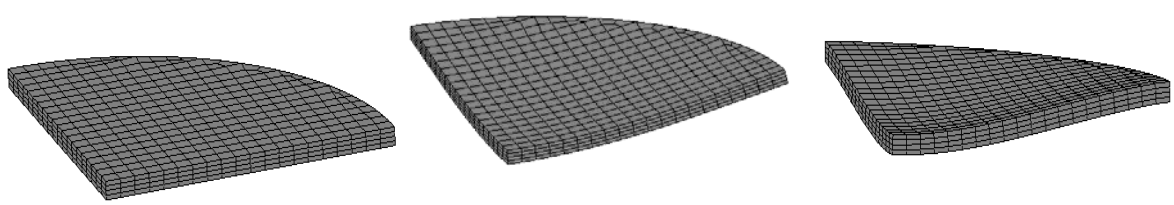

Figure 10: Mesh: a) circular slab, b) simple supported and c) fixed.

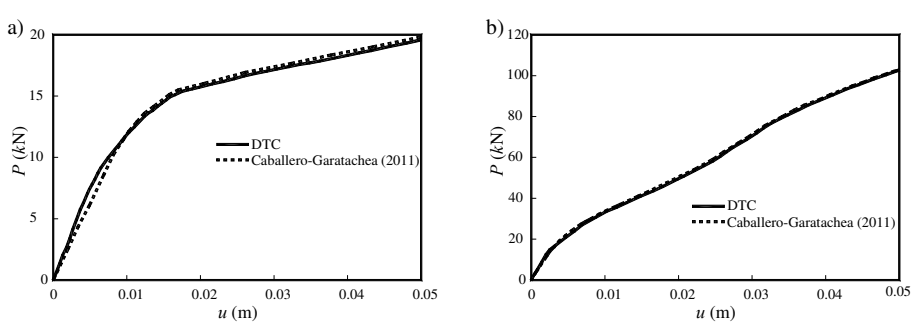

Figure 11: Load *vs.* displacement curves at the circular slab: a) simple supported and b) fixed.

3.3 Reinforced concrete deep beam

In this example, a reinforced concreted deep beam ($l/h=1$) is analysed, where a distributed uniformed load, with magnitude $q=0.0078125P$, is gradually applied downwards on the top of the beam shown in Figure 12a. The mechanical properties of the concrete are: Young's modulus $E_c=31400$ *MPa*, Poisson ratio $\nu=0.2$, ultimate tensile strength $\sigma_{tu}=2.5$ *MPa*, ultimate compressive strength $\sigma_{tu}=29.63$ *MPa* and fracture energy density $G_f=0.098$ *N/mm*. The mechanical properties of the steel reinforcement are: Young's modulus $E_s=206$ *GPa*, yield stress $\sigma_y=536.6$ *MPa*, Poisson ratio ν=0.3, area of the principal reinforcement bars $A_1=0.503$ cm^2 and the secondary reinforcement bars $A_2=0.178$ cm^2 and hardening modulus $H=2.871$ *GPa*. The distribution of the reinforcement is shown in Figure 12b.

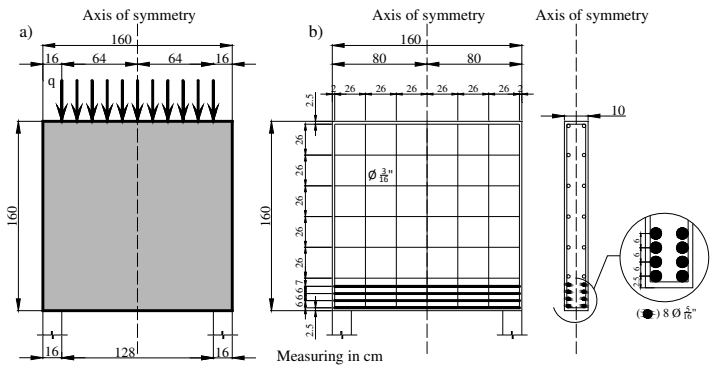

Figure 12: Deep beam: a) geometry and b) reinforcement.

In this example, an elastoplastic constitutive model was assigned to the steel as Leonhardt and Walther (1966) did. Taking advantage of the symmetry, only a quarter of the beam was modelled to reduce the time consuming computational cost. Figure 13 shows the 3D mesh, discretized with hexahedral elements.

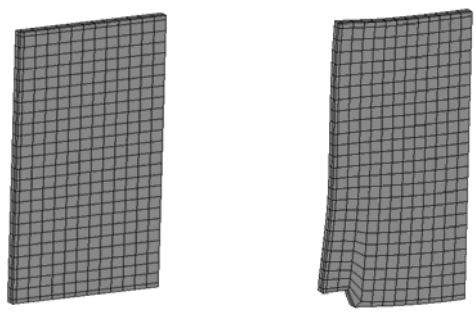

(a) **(b)**

Figure 13: Mesh: a) undeformed and b) deformed.

Figure 14 shows a comparative between the computed load-displacement curve and the experimental curve reported by Leonhardt and Walther (1966). It is observed that the numerical results are congruent whit the experimental results.

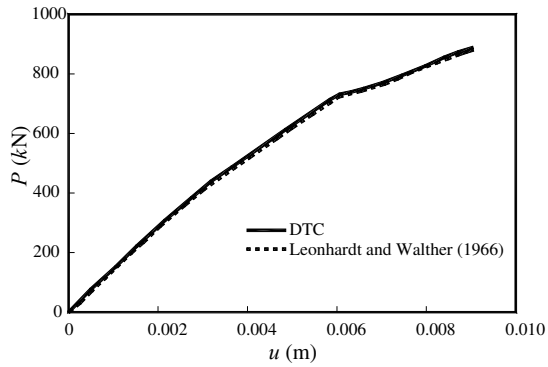

Figure 14: Load *vs.* displacement curves.

4 CONCLUSIONS

A damage model to simulate concrete elements to collapse was developed, implemented and validated, based on the damage mechanics continuous theory. The damage model considers a constitutive behaviour equipped with softening for the concrete elements limited for a damage surface, whereas for the reinforced concreted elements, a plasticity model was assigned to the reinforcement, which take into account the hardening of the steel with a Von Mises surface.

A DTC damage surface for concrete is obtained by scaling down the norm and the tangent modulus with the parameter χ, but it is equivalent by scaling up the threshold value of r_o. In both cases, the integration algorithm of the ETC damage model needs two and one modification, respectively, to have a surface with different threshold values in tension and compression.

The global behaviour of reinforced concrete elements is controlled by the hardening of the reinforcement steel. Their simulation with damage models for concrete and plasticity model for the steel provides the cracking zones, the crack paths and the ultimate load of the specimen.

The numerical results computed with the DTC damage model are coherent with the experimental and numerical results reported in the scientific literature, since it properly simulates the strain softening of the concrete and localizes the degradation zones.

To consider perfect bond between steel reinforcement and concrete does not show evident effects in the presented numerical examples.

It is useful over some commercial software that it is possible to assign the fracture energy density value in the implemented damage model, because the numerical results are dependent on this value.

The implemented damage model did not show the stress locking problem, a fact that guaranties a suitable simulation of the plain and reinforced concrete elements in their evolution to collapse.

Acknowledgements

The authors acknowledge the support given by the Universidad Autonoma Metropolitana. The first author acknowledges the financial support by CONACYT under the agreement number I010/176/2012 with the Universidad Autónoma Metropolitana, in the context of the research project: "Analysis and design of concrete slabs". The second author acknowledges the scholarship for his Master given by CONACYT.

References

ANSYS, (2009). Ansys 12.0.1. Ansys Inc. USA.

Armero, F., Garikipati, K. (1996). An analysis of strong discontinuities in multiplicative finite strain plasticity and their relation with the numerical simulation of strain localization in solids, International Journal of Solids and Structures 33(20): 2863-2885.

Bazant, Z., Oh, B.H. (1983). Crack band theory for fracture of concrete, Materials and Structures 16(3): 155-177.

Burns, N.H., Seiss, C.P. (1962). Load-deformation characteristics of beam-column connections in reinforced concrete, Technical Report Civil Engineering Studies SRS-234, Civil Engineering Department, University of Illinois at Urbana-Champaign, USA.

Caballero, O. (2012). Determinación de coeficientes de diseño y trayectorias de agrietamiento de losas circulares, elípticas y triangulares en condición aislada, Master thesis, Universidad Autónoma Metropolitana, Azcapotzalco, Mexico. (In Spanish).

Carol, I., Rizzi, E., William, K.J. (2001). On the Formulation of anisotropic elastic degradation. I. Generalized pseudo-Rankine model for tensile damage, International Journal of Solids and Structures 38(4): 519-546.

Cicekli, U., Voyiadjis, G.Z., Abu Al-Rub, R.K. (2007). A plasticity and anisotropic damage model for plain concrete, International Journal of Plasticity 23(10-11): 1874-1900.

Comi, C. (2001). A non-local model with tension and compression damage mechanisms, European Journal of Mechanics - A/Solids 20(1) 1-22.

Contrafatto, L., Cuomo, M. (2006). A framework of elastic-plastic damaging model for concrete under multiaxial stress states - International Journal of Plasticity, 22(12): 2272-2300.

Cordebois, J.P., Sidoroff, F. (1979). Anisotropic damage in elasticity and plasticity, Journal de Mecanique Theorique et Applilquee, Special number, 45-40.

Costa Mattos, H., Fremond, M., Mamiya, E. N. (1992). A simple model of the mechanical behavior of ceramic-like materials, International Journal of Solids and Structures 29(24): 3185–3200.

Costa Mattos, H.S., Sampaio R. (1995). Analysis of the fracture of brittle elastic materials using a continuum damage model, Structural Engineering and Mechanics 3(5): 411–427.

Crisfield, M.A. (1986). Snap-through and snap-back response in concrete structures and the dangers of under integration, International Journal for Numerical Methods in Engineering 22(3): 751-756.

Da Costa-Mattos, H., Pires-Domingues, S.M., Alves Rochinha, F. (2009). Structural failure prediction of quasi-brittle structures: Modeling and simulation, Computational Materials Science 46(2): 407-417.

de Borst, R. (1991). Simulation of strain localization: a reappraisal of the Cosserat continuum, Engineering Computations 8(4): 317-332.

de Borst, R., Mühlhaus, H.B. (1992). Gradient-dependent plasticity: formulation and algorithmic aspects, International Journal for Numerical Methods in Engineering 35(3): 521-539.

DIANA (2008), DIANA 9.0: Finite Element Analysis User's Manual Release. TNO DIANA BV, Delft, The Netherlands.

Dragon, A., Mroz, Z. (1979). A continuum model for plastic-brittle behavior of rock and concrete, International Journal of Engineering Science 17(2): 121-137.

Faria, A., Oliver, J., Cervera, M. (1998). A strain-based plastic viscous-damage model for massive concrete structures, International Journal of Solids and Structures 35(14): 1533-1558.

Fichant, S., Borderie, C.L., Pijaudier-Cabot, G. (1999). Isotropic and anisotropic descriptions of damage in concrete structures, Mechanics of Cohesive-frictional Materials 4(4): 339-359.

Gopinath, S., Rajasankar, J., Iyer, N.R. (2012). Nonlinear analysis of RC structures using isotropic damage model, International Journal of Damage Mechanics 21(5): 647-669.

Govindjee, S., Kay, G.J., Simo, J.C. (1995). Anisotropic modelling and numerical simulation of brittle damage in concrete, International Journal for Numerical Methods in Engineering 38(21): 3611-3633.

Halm, D., Dragon, A. (1996). A model of anisotropic damage by mesocrack growth; unilateral effect, International Journal of Damage Mechanics 5(4): 384-402.

Hillerborg, A., Modeer, M., Petersson, P.E. (1976). Analysis of crack formation and crack growth in concrete by means of fracture mechanics and finite elements, Cement and Concrete Research 6(6): 773-782.

Jason, L., Huerta, A., Pijaudier-Cabot, G., Ghavamian, S. (2006). An elastic plastic damage formulation for concrete: Application to elementary tests and comparison with an isotropic damage model, Computer Methods in Applied Mechanics and Engineering 195(52): 7077-7092.

Jirásek, M. (1998). Nonlocal models for damage and fracture: Comparison of approaches, 35(31–32): 4133–4145.

Ju, J.W. (1989). On energy-based coupled elasto-plastic damage theories, constitutive modeling and computational aspects, International Journal of Solids and Structures 25(7): 803-833.

Ju, J.W. (1990). Isotropic and anisotropic damage variables in continuum damage mechanics, ASCE Journal of Engineering Mechanics 116(12): 2764-2770.

Juárez, G., Ayala, G.A. (2009). Variational formulation of the material failure process in solids by embedded discontinuities model, Numerical Methods for Partial Differential Equations 25(1): 26-62.

Juárez-Luna, G., Ayala, G.A. (2014). Improvement of some features of finite elements with embedded discontinuities, Engineering Fracture Mechanics 118: 31-48.

Kachonov, L.M. (1958). On the creep fracture time, Izv. Akad. Nauk USSR Otd. Tech. 8: 26-31. (in Russian).

Krajcinovic, D. (1984). Continuum damage mechanics, Applied Mechanics Reviews 37(1): 1-6.

Krajcinovic, D. (1985). Continuous damage mechanics revisited: basic concepts and definitions, Journal of Applied Mechanics 52(4): 829-834.

Krajcinovic, D., Fonseka, G.U. (1981). The continuous damage theory of brittle materials. Part I: general theory, Journal of Applied Mechanics 48(4): 809-815.

Kupfer, H.B., Gerstle, K.H. (1973). Behavior of concrete under biaxial stresses, ASCE Journal of Engineering Mechanics 99(4): 853-866.

Lee, J., Fenves, G.L. (1998). Plastic-damage model for cyclic loading of concrete structures, ASCE Journal of Engineering Mechanics 124(8): 892-900.

Lemaitre, J. (1986). Local approach to fracture, Engineering Fracture Mechanics 25(56): 523-537.

Lemaitre, J., Demorat, Sauzay, R.M. (2000). Anisotropic damage law of evolution, European Journal of Mechanics - A/Solids 19(2): 513-524.

Leonhardt, F., Walther, R. (1966). Wandartige Trager. Deutscher Ausschuss für Stahlbeton, Berlin, Heft 178.

Linero, D.L. (2006). Un modelo del fallo material en el hormigón armado, mediante la metodología de discontinuidades fuertes de continuo y la teoría de mezclas. Dissertation, Escola Tècnica Superior d'Enginyers de Camins, Canals i Ports, Universidad Politécnica de Cataluña, Spain. (In Spanish).

Lubarda, V.A., Kracjinvovic, D., Mastilovic, S. (1994). Damage model for brittle elastic solids with unequal tensile and compressive strength, Engineering Fracture Mechanics 49(5): 681-697.

Lubliner, J., Oliver, J., Oller, S., Onate, E. (1989). A plastic-damage model for concrete, International Journal of Solids and Structures 25(3): 299-326.

Mazars, J., Pijaudier-Cabot, G., (1989). Continuum damage theory: Application to concrete, ASCE Journal of Engineering Mechanics 115(2): 345-365.

Méndez-Martínez H., Juárez-Luna, G. (2012). Implementación de un modelo de daño continuo para la simulación al colapso de estructuras de concreto, Concreto y Cemento. Investigación y Desarrollo, Instituto Mexicano del Cemento y del Concreto A.C., 3(2): 19-33. (In Spanish).

Needleman, A. (1988). Material rate dependence and mesh sensitivity in localization problems, Computer Methods in Applied Mechanics and Engineering 67(1): 69-87.

Oliver, J. (1989). A consistent characteristic length for smeared cracking models, International Journal for Numerical Methods in Engineering 28(2): 461-474.

Oliver, J., Cervera, M., Oller, S., Lubliner, J. (1990). Isotropic damage models and smeared crack analysis of concrete. In N. B. *et al.*, Eds, SCI-C Computer Aided Analysis and Design of Concrete Structures, Swansea, Pineridge Press, 945-957.

Oliver, J. (1996a). Modelling strong discontinuities in solid mechanics via strain softening constitutive equations, Part 1: Fundamentals, International Journal for Numerical Methods in Engineering 39(21): 3575-3600.

Oliver, J. (1996b). Modelling strong discontinuities in solid mechanics via strain softening constitutive equations. Part 2: Numerical simulation, International Journal for Numerical Methods in Engineering 39(21): 3601-3623.

Oliver, J., Huespe, A.E., Pulido, M.D.G., Chaves, E. (2002). From continuum mechanics to fracture mechanics: the strong discontinuity approach, Engineering Fracture Mechanics 69(2): 113-136.

Ortiz, M. (1985). A constitutive theory for the inelastic behavior of concrete, Mechanics of Materials 4(1): 67-93.

Peerlings, R.H.J., De Borst, R., Brekelmans, W.A.M., De Vree J.H.P. (1996). Gradient enhanced damage for quasi-brittle materials, International Journal for Numerical Methods in Engineering 39(19): 3391-3403.

Rashid, Y.R. (1968). Ultimate strength analysis of prestressed concrete pressure vessels, Nuclear Engineering and Design 7(4): 334-344.

Rots, J.G. (1988). Computational modeling of concrete fracture, Dissertation, Delft University of Technology, Delft, Netherlands.

Simo, J.C., Ju, J.W. (1987a). Strain and stress based continuum damage models. I. Formulation, International Journal of Solids and Structures 23(7): 821-840.

Simo, J.C., Ju, J.W. (1987b). Strain- and stress-based continuum damage models. Part II: Computational aspects, International Journal of Solids and Structures 23(7): 841-869.

Simo, J.C., Oliver, J., Armero, F. (1993). An analysis of strong discontinuities induced by strain-softening in rate-independent inelastic solids, Computatlonal Mechanics 12: 277-296.

Steinmann, P. (1995). Theory and numerics of ductile micropolar elastoplastic damage, International Journal for Numerical Methods in Engineering 38(4): 583-606

Taylor, R.L. (2008). A Finite Element Analysis Program, Version 8.2. Department of Civil and Environmental Engineering, University of California, Berkeley.

Triantafylidis, N., Aifantis, E. C. (1986). A gradient approach to localization of deformation. I. Hyperelastic materials, Journal of Elasticity 16(3): 225-237.

Voyiadjis, G.Z., Abu-Lebdeh, T.M. (1994). Plasticity model for concrete using the bounding surface concept, International Journal of Plasticity 10(1): 1-21.

Wu, J.U., Li, J., Faria, R. (2006). An energy release rate-based plastic-damage model for concrete, International Journal of Solids and Structures 43(3-4): 583-612.